

*Alexander Velichenko<sup>1</sup>, Valentina Krysh<sup>1</sup>, Tatiana Luk'yanenko<sup>1</sup>,  
Larisa Dmitrikova<sup>2</sup>, Yulia Velichenko<sup>2</sup> and Didier Devilliers<sup>3</sup>*

## **PbO<sub>2</sub> BASED COMPOSITE MATERIALS DEPOSITED FROM SUSPENSION ELECTROLYTES: ELECTROSYNTHESIS, PHYSICO-CHEMICAL AND ELECTROCHEMICAL PROPERTIES**

<sup>1</sup>*Department of Physical Chemistry, Ukrainian State University of Chemical Technology  
8, Gagarin ave., 49005 Dnepropetrovsk, Ukraine;*

<sup>2</sup>*Department of Organic Chemistry, Dnepropetrovsk National University  
13, Nauchnaya str., 49000 Dnepropetrovsk, Ukraine*

<sup>3</sup>*Université Pierre et Marie Curie, Laboratoire PECSA – UMR 7195 UPMC-CNRS-ESPCI  
4, Place Jussieu, 75252 Paris Cedex 05, France*

*Received: July 03, 2011 / Revised: July 08, 2011 / Accepted: September 22, 2011*

© Velichenko A., Krysh V., Luk'yanenko T., Dmitrikova L., Velichenko Yu., Devilliers D., 2012

**Abstract.** Composite materials based on PbO<sub>2</sub> containing TiO<sub>2</sub> or ZrO<sub>2</sub> were prepared from electrolytes containing a suspension of TiO<sub>2</sub> or ZrO<sub>2</sub>. The contents of foreign oxides in the composite depend on the electrolyte composition and conditions of deposition. When a dispersed phase is incorporated into the composite coating, the dimensions of lead dioxide crystals decrease to submicro- and nano-size. Physico-chemical properties and electrocatalytic activity of composite materials are mainly determined by their chemical composition. The electrocatalytic properties of a composite PbO<sub>2</sub>-TiO<sub>2</sub> anode vs the oxygen evolution reaction (OER) and the electrochemical degradation of methyl *tert*-butyl ether (MTBE) were investigated.

**Keywords:** electrodeposition, suspension, composite, PbO<sub>2</sub>, TiO<sub>2</sub>, ZrO<sub>2</sub>, MTBE.

### **1. Introduction**

Anodes based on oxide composite materials have wide use in various reactions as photo- and electrocatalysts, in electrochemical synthesis of strong oxidizing agents, in electrochemical removal of organic and inorganic contaminants in water [1-6]. Various ways to produce materials of this type are known, *e.g.*, sol-gel techniques, plasmochemical method, and so on. The electrochemical method should be distinguished as one of the most promising because it enables wide control over the composition and properties of composites due to its simple implementation and possibility of smoothly varying the technological parameters of the process [7-9].

Lead dioxide is a promising material widely used in different applications [10-13]. Electrodeposited pure lead dioxide was demonstrated to exhibit a moderate electrocatalytic activity toward various anodic reactions in acidic media. However, this activity can often be enhanced greatly by incorporation of some ions, for example Bi<sup>3+</sup>, As<sup>3+</sup>, Fe<sup>3+</sup>, Cl<sup>-</sup>, F<sup>-</sup> [13]. There is much less information on effects of polyelectrolyte and surfactant additives on the process of oxide electrodeposition and the physicochemical properties of the resulting materials. It was shown [13] that both polyelectrolytes and anionic surfactants are adsorbed on PbO<sub>2</sub> and that the composite materials prepared from plating solutions containing those additives have new physicochemical properties.

Composite materials based on lead dioxide and containing various oxides have been reported in literature, in particular: Al<sub>2</sub>O<sub>3</sub>, Co<sub>3</sub>O<sub>4</sub>, RuO<sub>2</sub>, TiO<sub>2</sub> and ZrO<sub>2</sub> [4, 8, 9, 14]. In this study, the fundamental aspects of electrodeposition of PbO<sub>2</sub>-TiO<sub>2</sub> and PbO<sub>2</sub>-ZrO<sub>2</sub> composites are examined, as well as the physicochemical and electrocatalytic properties of these materials.

### **2. Experimental**

The composites were deposited in the galvanostatic mode onto pretreated platinum-plated titanium electrodes of the area 4 cm<sup>2</sup>. The deposition electrolyte contained 0.1M Pb(NO<sub>3</sub>)<sub>2</sub> and 0.1M HNO<sub>3</sub>. Additionally, TiO<sub>2</sub> (35 nm) or ZrO<sub>2</sub> (26 nm) powder was added into the electrolyte. Titanium and zirconium dioxide powders are monodispersed particles according to the producer data

(Crimean Titanium Inc., Ukraine). In some cases we used an anionic surfactant: sodium dodecylsulfate  $C_{12}H_{25}SO_4Na$  (SDS) as an additive into the electrolyte. Solutions were prepared from reagents of chemically pure grade and twice-distilled water. The deposition was performed (in most cases) at the temperature of  $293 \pm 2$  K and anode current density of  $5 \text{ mA/cm}^2$ ; the coating deposition time was 30 min. To study the physicochemical properties of the composites, thicker coatings were deposited (deposition time 2 h). It should be noted that the composite materials under study had the composition independent of the coating thickness. For instance, we deposited the composite from the same electrolyte and conditions at 30, 60, 120, 180 min and the coating composition was the same in all cases.

The adsorption of SDS on  $TiO_2$  and  $ZrO_2$  powder was studied in 0.1M HCl. Adsorption of  $Pb^{2+}$  on  $TiO_2$  or  $ZrO_2$  in 0.1M  $HNO_3$  + xM  $Pb(NO_3)_2$  was performed according to the following procedure: 0.2 g of the oxide powder was added to 15 ml of  $Pb^{2+}$  solutions of different concentrations. After one day the equilibrium concentration of  $Pb^{2+}$  in the solutions was determined by amperometric titration with diethylthiocarbamate. Adsorption was calculated as the difference between the initial and equilibrium concentration of  $Pb^{2+}$  in the solution.

The electrokinetic potential was measured using the electrophoretic technique. The electrophoresis was performed in a U-shaped tube with platinum electrodes ( $\Delta E = 100$  V). The point of zero charge ( $pH_0$ ) was measured in 0.1M KCl.

The total amount of deposited material was determined by the increase of the weight of the electrode. After the experiments, the materials were dissolved in a 1:1 mixture of 5M  $HNO_3$  and 30% hydrogen peroxide. The excess of  $H_2O_2$  in the resulting solutions was removed by boiling with a platinum catalyst. The initial amount of  $PbO_2$  was calculated from the  $Pb^{2+}$  content of the solution, found by amperometric titration with sodium diethyldithiocarbamate trihydrate –  $(C_2H_5)_2NCS_2Na \cdot 3H_2O$ , whereas the amount of  $TiO_2$  or  $ZrO_2$  was deduced by subtraction.

The surface morphology of the materials obtained was studied by scanning electron microscopy (SEM) with a LEICA S360 microscope. X-ray diffraction patterns were recorded with a PHILIPS PW3710 diffractometer

(Cu  $K\alpha$  radiation). The deposits were cleaned ultrasonically before all measurements.

Accelerated tests for determination of anodes service life were performed in 1M  $H_2SO_4$  at anodic current density of  $200 \text{ mA/cm}^2$ . Oxygen evolution reaction was studied in 1M  $H_2SO_4$ . Electrooxidation of methyl *tert*-butyl ether (MTBE) was studied in a divided cell on  $PbO_2$ - $TiO_2$  anodes (the electrode area was  $2 \text{ cm}^2$ ) in the electrolyte of the initial composition of 0.5M  $Na_2SO_4$  + buffer phosphate +  $2 \cdot 10^{-2}$ M MTBE ( $pH = 6.68$ ). Electrolysis was carried out in a cell in which the anodic and cathodic compartments were separated by a Nafion<sup>®</sup> membrane. The volume of anolyte was 160 ml, anodic current density was  $50 \text{ mA/cm}^2$ . A 15W low pressure UV lamp emitting a wavelength of 254 nm was situated parallel to the electrode.

A CHROM 5 gas chromatograph equipped with a SE-30 column (polyethylene glycol saturated by ferrochromium) with a length of 2.5 m and an ID of 3 mm and a flame ionization detector was used for solution analyses. The oven temperature was 343 K. The carrier gas was argon at a flow rate of 25 ml/min. Sampling was performed at 0, 30, 60, 90, 120, 150, 180, 210, 240, 270 and 300 min. (each kinetic curve consists of 11 points). The experiments have been performed 3 times in order to verify the reproducibility of the results. The constant rates were calculated from the experimental kinetic curves ( $\ln C = f(t)$  for the first order reaction) using linear regression procedure. Correlation coefficient was in the range of 0.990–0.998 and the maximum standard error was  $5 \cdot 10^{-4}$ .

### 3. Results and Discussion

#### 3.1. Colloidal-Chemical Properties of Suspensions

The composition of composite materials, which are fabricated by electrochemical methods, is determined to a large extent by the nature and colloidal-chemical properties of the suspension electrolyte. The dimension of dispersed phase particles, the electrokinetic potential, and the point of zero-charge  $pH_0$  of oxide are the main characteristics of the suspension electrolyte.

Table 1

**The size of aggregates in the suspension (for the main fraction)**

No.	MO <sub>2</sub> -Suspension composition (M = Ti or Zr)	Particle size, nm	
		TiO <sub>2</sub>	ZrO <sub>2</sub>
1	H <sub>2</sub> O + 2.0 g/dm <sup>3</sup> MO <sub>2</sub>	35	26
2	0.1 M HNO <sub>3</sub> + 0.1 M Pb(NO <sub>3</sub> ) <sub>2</sub> + 2.0 g/dm <sup>3</sup> MO <sub>2</sub>	1040	578
3	0.1M HNO <sub>3</sub> + 0.1 M Pb(NO <sub>3</sub> ) <sub>2</sub> + $3 \times 10^{-4}$ M C <sub>12</sub> H <sub>25</sub> SO <sub>4</sub> Na + 2.0 g/dm <sup>3</sup> MO <sub>2</sub>	1950	732

The size of dispersed phase particles in the suspension was determined sedimentometrically. Addition of electrolytes and the surfactant in the suspension led to a particle aggregation. It was found that in these cases the systems are polydispersed. According to the data presented in Table 1 the size of aggregate of the main fraction increases dramatically in the presence of Pb<sup>2+</sup> and SDS in the suspension electrolyte and it depends on the nature of the oxide of the dispersed phase. According to DLVO (Derjaguin, Landau, Verwey, Overbeek) theory the compression of the double layer with the increasing electrolyte concentration has dramatic effects on the stability of colloidal dispersions. At low electrolyte concentration, the atmosphere of counterions is extended, and particles are widely separated. Higher electrolyte concentrations compress the diffuse layer, and the particles approach more closely. The dispersion also becomes unstable when the surface charge disappears. This occurs when the concentration of potential-determining ions is changed or when strongly adsorbed counterions are introduced.

When the Pb<sup>2+</sup> ions are introduced into the deposition electrolyte, they are adsorbed on TiO<sub>2</sub> and ZrO<sub>2</sub> particles (Fig. 1). The adsorption of Pb<sup>2+</sup> ions on the TiO<sub>2</sub> and ZrO<sub>2</sub> powder has a specific character and it is the result of the ionic-exchange reaction of divalent metal ion with adsorption sites on the oxide. It is important to note that at typical concentration of Pb<sup>2+</sup> in the suspension electrolyte (0.1M) the coverage of adsorbed ions on the oxides is very high ( $\theta = 0.7$  for TiO<sub>2</sub> and  $\theta = 0.3$  for ZrO<sub>2</sub>).

The adsorption of SDS (Fig. 2) is satisfactorily described by the Frumkin isotherm:

$$Bc = \frac{q}{1-q} \exp(-2aq) \quad (1)$$

where:  $c$  – equilibrium concentration;  $B$  – adsorption constant;  $\theta = \frac{A}{A_{\infty}}$ ;  $A$  – adsorption;  $A_{\infty}$  – limiting adsorption;  $a$  – attraction constant.

Free adsorption energy ( $\Delta G$ ) was calculated from the equation:

$$B = 0.018 \exp(-\Delta G / RT) \quad (2)$$

Adsorption of SDS on TiO<sub>2</sub> and ZrO<sub>2</sub> has the following parameters: for TiO<sub>2</sub>, the limiting adsorption  $A_{\infty} = 1.75 \cdot 10^{-5}$  mol/g, reached for a SDS concentration of  $3.8 \cdot 10^{-4}$  M, and the adsorption constant  $B = 673.81$  1/M; for ZrO<sub>2</sub>, the limiting adsorption  $A_{\infty} = 1.20 \cdot 10^{-5}$  mol/g, reached for [SDS] =  $4 \cdot 10^{-4}$  M and adsorption constant  $B = 132.9$  1/M. The adsorption of SDS on the TiO<sub>2</sub> and ZrO<sub>2</sub> powder has a weak specific nature, which is indicated by the rather low value of the adsorption interaction energy  $\Delta G = -25.6$  kJ/mol and  $-21.7$  kJ/mol,

respectively. According to the presented data, adsorption of the surfactant on TiO<sub>2</sub> is stronger than that on ZrO<sub>2</sub>.

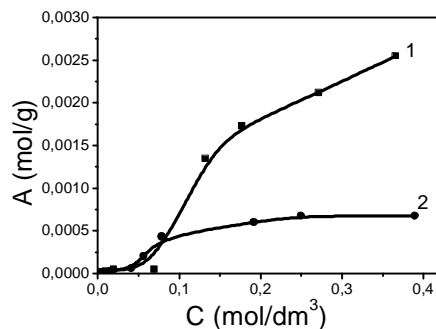


**Fig. 1.** Adsorption of Pb<sup>2+</sup> on different oxides: ZrO<sub>2</sub> (1) and TiO<sub>2</sub> (2).  $C$  is the equilibrium concentration of Pb<sup>2+</sup> in the solution;  $A$  is the adsorption of Pb<sup>2+</sup> on the ZrO<sub>2</sub> or TiO<sub>2</sub> particles

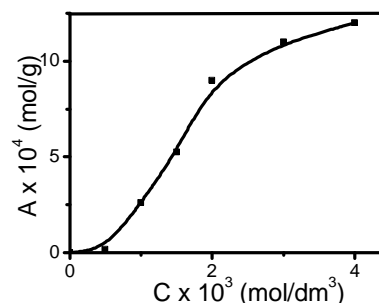


**Fig. 2a.** Adsorption of SDS on ZrO<sub>2</sub>

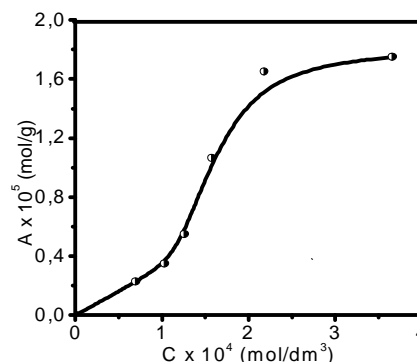


**Fig. 2b.** Adsorption of SDS on TiO<sub>2</sub>

One of the factors affecting the supply rate of the inert oxide to the electrode surface is the charge of particles in the dispersed phase. According to potentiometric data,  $pH_0$  for TiO<sub>2</sub> and ZrO<sub>2</sub> is 6.36 and 6.82 respectively; therefore, dispersed phase particles are positively charged in the acidic suspension electrolyte. When the adsorption of a surfactant occurs on oxides, the point of zero charge is shifted to the alkaline region, which confirms the conclusion about the specific nature of SDS adsorption on particles of the dispersed phase.

Measurements demonstrated that the electrokinetic potential ( $\zeta$ ) of  $\text{TiO}_2$  and  $\text{ZrO}_2$  in 0.1M  $\text{HNO}_3$  is 0.064 V and 0.096 V, respectively. The low value of  $\zeta$  is due to the high concentration of supporting electrolyte. When SDS is added, the electrokinetic potential substantially changes to become -0.18 V and -0.24 V for  $\text{TiO}_2$  and  $\text{ZrO}_2$ , respectively. The change in the sign and magnitude of the electrokinetic potential upon addition of SDS indicates that the electric double layer of particles of the dispersed phase is recharged (surface charge is changed from positive to negative) because of the adsorption of the surfactant. In the presence of the anionic surfactant, particles of the dispersed phase acquire a negative charge and can migrate toward the positively charged anode surface via electrophoresis.

### 3.2. Electrodeposition of Composites

According to the data presented in the previous section the electrolytes remain stable only during the 30-min electrolysis if unstirred. However, for investigating the physicochemical properties of composite materials, a longer time of electrolysis is required, in which the suspension is partially broken. In order to avoid a change of the electrolyte composition with time and to standardize the conditions of deposition, in all cases the composite materials were prepared under stirring with a magnetic stirrer at constant rotation speed.

Particles of the dispersed phase are incorporated into the growing  $\text{PbO}_2$  deposit to give a composite material. The content of  $\text{TiO}_2$  and  $\text{ZrO}_2$  in the composite will be determined by the way in which particles of the dispersed phase are delivered from the electrolyte bulk to the electrode surface. As the potential of the zero charge of lead dioxide in 0.1M  $\text{HNO}_3$  is  $0.91 \pm 0.1$  V (relative to

the standard calomel electrode) at the deposition potentials the electrode surface will be positively charged. For the experiments without SDS,  $\text{TiO}_2$  and  $\text{ZrO}_2$  particles of the dispersed phase are transported to the electrode, despite their positive charge, due to the convective-diffusion. For the experiments with SDS in the suspension, the additional contribution of the migration of the negative  $\text{TiO}_2$  and  $\text{ZrO}_2$  particles towards the anode is expected.

The amount of particles in the solution has a significant effect on the percentage volume fraction of the particles incorporated into the oxide deposits (Fig. 3).

Two general observations can be made: (1) the volume fraction of particles in the oxide deposit increases substantially when the amount of particles in the solution increases and (2) a saturation state of particles in the deposit is reached at high particle amount in the solution. It is important to note that at the same content of oxides in the electrolyte the amount of  $\text{ZrO}_2$  into the composite is higher than that of  $\text{TiO}_2$ . It is due to lower size of  $\text{ZrO}_2$  particles (Table 1) and their higher number in the suspension. The coating composition also depends on the solution pH and temperature. An increase in the  $\text{HNO}_3$  concentration leads to a decrease of the oxide content into the composite (Fig. 4), which is due to a rise in the positive charge of particles of the dispersed phase and to an increase in the rate of migration of oxide particles into the cathode space.

As the deposition temperature is raised, the content of particles of the dispersed phase in the coating decreases (Fig. 5) because of a decrease in the viscosity of the electrolyte, which, in turn, results in a decrease of the amount of particles near electrode in the suspension due to the sedimentation.

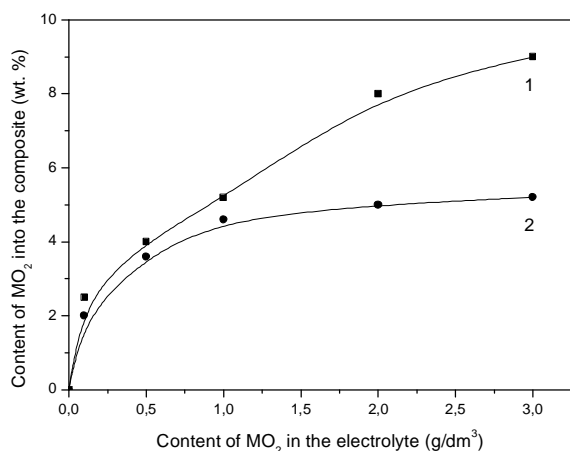


**Fig. 3.** Effect of the amount of foreign oxides ( $\text{MO}_2$ ) in the electrolyte on their content in the composite material deposited from the solution of 0.1M  $\text{HNO}_3$  + 0.1M  $\text{Pb}(\text{NO}_3)_2$  +  $x$   $\text{g/dm}^3$   $\text{MO}_2$  at anodic current density of 5  $\text{mA/cm}^2$ , where  $\text{MO}_2$  is  $\text{ZrO}_2$  (1) and  $\text{TiO}_2$  (2)

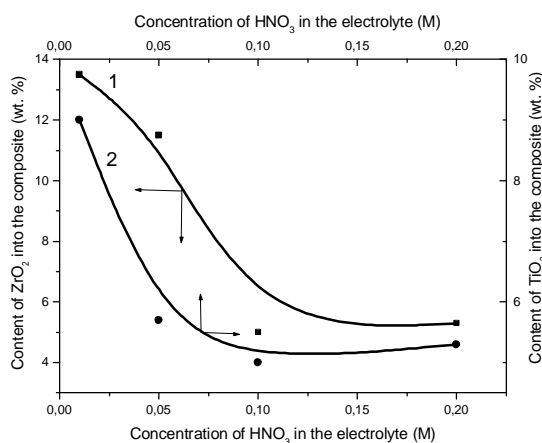


**Fig. 4.** Effect of  $\text{HNO}_3$  concentration in the electrolyte on the foreign oxide content in the composite material deposited at anodic current density of 5  $\text{mA/cm}^2$  from different solutions:  $x$ M  $\text{HNO}_3$  + 0.1M  $\text{Pb}(\text{NO}_3)_2$  + 1.0  $\text{g/dm}^3$   $\text{ZrO}_2$  (1) and  $x$ M  $\text{HNO}_3$  + 0.1M  $\text{Pb}(\text{NO}_3)_2$  + 2.0  $\text{g/dm}^3$   $\text{TiO}_2$  (2)

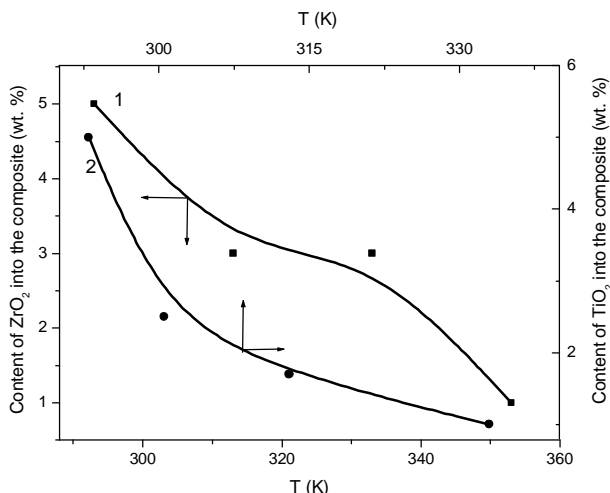


**Fig. 5.** Effect of temperature on the foreign oxide content in the composite material deposited at anodic current density of 5 mA/cm<sup>2</sup> from different solutions: 0.1M HNO<sub>3</sub> + 0.1M Pb(NO<sub>3</sub>)<sub>2</sub> + 1.0 g/dm<sup>3</sup> ZrO<sub>2</sub> (1) and 0.1M HNO<sub>3</sub> + 0.1M Pb(NO<sub>3</sub>)<sub>2</sub> + 2.0 g/dm<sup>3</sup> TiO<sub>2</sub> (2)

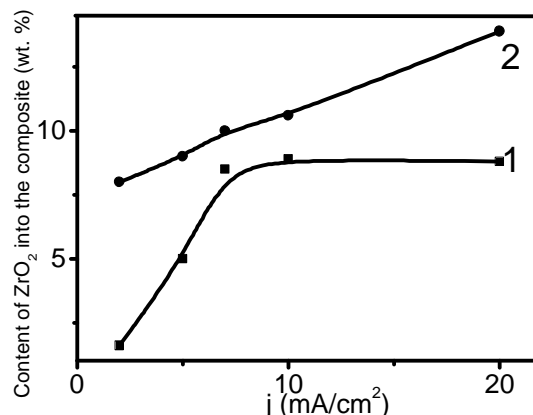


**Fig. 6a.** Effect of deposition current density (*j*) on the ZrO<sub>2</sub> content in the composite material deposited from different solutions: 0.1M HNO<sub>3</sub> + 0.1M Pb(NO<sub>3</sub>)<sub>2</sub> + 1.0 g/dm<sup>3</sup> ZrO<sub>2</sub> (1) and 0.1M HNO<sub>3</sub> + 0.1M Pb(NO<sub>3</sub>)<sub>2</sub> + 1.0 g/dm<sup>3</sup> ZrO<sub>2</sub> + 7·10<sup>-4</sup>M SDS (2)

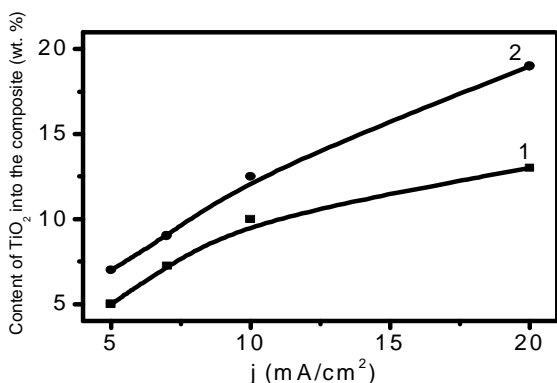


**Fig. 6b.** Effect of deposition current density (*j*) on the TiO<sub>2</sub> content in the composite material deposited from different solutions: 0.1M HNO<sub>3</sub> + 0.1M Pb(NO<sub>3</sub>)<sub>2</sub> + 2.0 g/dm<sup>3</sup> TiO<sub>2</sub> (1) and 0.1M HNO<sub>3</sub> + 0.1M Pb(NO<sub>3</sub>)<sub>2</sub> + 2.0 g/dm<sup>3</sup> TiO<sub>2</sub> + 7·10<sup>-4</sup>M SDS (2)

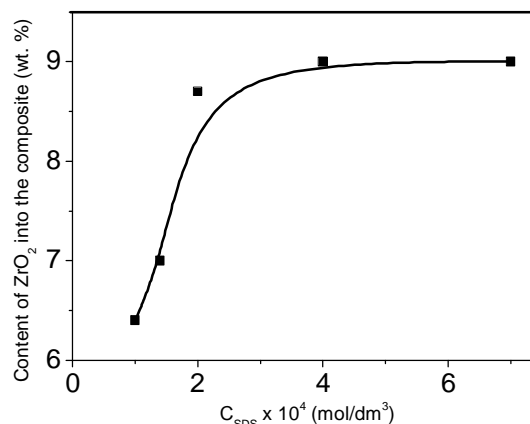


**Fig. 7.** Effect of SDS concentration in the solution on the ZrO<sub>2</sub> content in the composite material deposited from 0.1M Pb(NO<sub>3</sub>)<sub>2</sub> + 0.1M HNO<sub>3</sub> + 1.0 g/dm<sup>3</sup> ZrO<sub>2</sub> + xM SDS

As the current density increases, the content of the inert oxide in the composite material grows (Fig. 6). The curve describing the content of the dispersed phase in the composite as a function of the current density can be divided into two portions. In the first region ( $j \leq 10 \text{ mA/cm}^2$ ) as the deposition rate of lead dioxide grows, the probability of capture of TiO<sub>2</sub> and ZrO<sub>2</sub> particles becomes higher and the content of the inert oxide in the composite increases. In the second region ( $j \geq 10 \text{ mA/cm}^2$ ), the content of TiO<sub>2</sub> and ZrO<sub>2</sub> in the coating remains nearly constant as soon as the deposition rate reaches its limiting value.

An important factor affecting incorporation of the inert oxide into an electrochemically grown film is the

charge of the particles of the dispersed phase. Anionic surfactants confer a net negative charge to the particles of dispersed phase, which attracts them electrostatically to the anode. According to data presented in Fig. 7, the content of ZrO<sub>2</sub> into the composite strongly depends on the concentration of SDS in the suspension electrolyte. It is important to note that observed dependence (Fig. 7) is rather similar to the adsorption isotherm of SDS on oxides of dispersed phase (Fig. 2).

When the surfactant is added into the deposition electrolyte, it is adsorbed on TiO<sub>2</sub> and ZrO<sub>2</sub>; thus, the surface of particles of the dispersed phase is recharged. In this case, negatively charged oxide-surfactant particles

move under the action of electrophoretic forces toward the positively charged anode to be incorporated there into the growing coating. In the presence of the additive, the content of particles of the inert oxide in the composite material also grows with the current density (Fig. 6), but the concentration of foreign oxide in the coating does not mainly approach a limiting value. In this case, particles of oxide are delivered not only by convective-diffusion, but also *via* migration which rate steadily increases as the polarization becomes more pronounced.

So, particles of the dispersed phase are incorporated into the growing  $\text{PbO}_2$  deposit to give a composite material, and the content of foreign oxide in the composite will be determined by the stages in which particles are delivered from the electrolyte bulk to the electrode surface. Additives introduced into the deposition electrolyte are adsorbed on oxides of the dispersed phase and cause the surface of particles of the dispersed phase to be recharged. The negatively charged oxide/surfactant particles are transported toward the positively charged electrode where, in this case, their incorporation into the growing coating is assisted by the electric field.

From a general point of view, the  $\text{TiO}_2$  and  $\text{ZrO}_2$  can be considered as electrochemically inert because their deposition does not require their oxidation/reduction, but they are not completely "inert", as they influence the deposition kinetics by providing extra nucleation sites like  $[\text{MO}_2]\text{Pb}^{2+}_{\text{ads}}$  or  $[\text{MO}_2]\text{OH}_{\text{ads}}$ . [14]. It means that in our case oxide of dispersed phase is involved in the electrochemical deposition of lead dioxide. Taking into account (i) the formation of colloidal  $\text{PbO}_2$  particles during the electrodeposition process [13, 14], (ii) the adsorption of negatively charged additives on  $\text{PbO}_2$ ,  $\text{TiO}_2$  and  $\text{ZrO}_2$  particles, and (iii) the influence of electrolysis conditions and electrolyte composition mentioned above, we can suggest the colloidal-electrochemical mechanism of the composite material formation [13-15].

### 3.3. Structure and Morphology of Composites

Lead dioxide obtained from acid nitrate solutions is a polycrystalline deposit composed of a mixture of  $\alpha$ - and  $\beta$ -phases with various crystallographic orientations, with the predominance of the latter phase [16]. The main orientations are (110), (011), (220), and (130) for  $\beta$ -phase, and (111) for  $\alpha$ -phase (Fig. 8a).

As was shown in [16], in some cases, the phase composition of lead dioxide coatings can depend on the deposit thickness. To avoid this undesirable effect, all measurements were performed on specimens with identi-

cal coating thickness. As can be seen from the X-ray diffraction patterns (Fig. 8b), the additions of  $\text{ZrO}_2$ ,  $\text{TiO}_2$  and surfactant have a pronounced effect on the structure of lead dioxide.

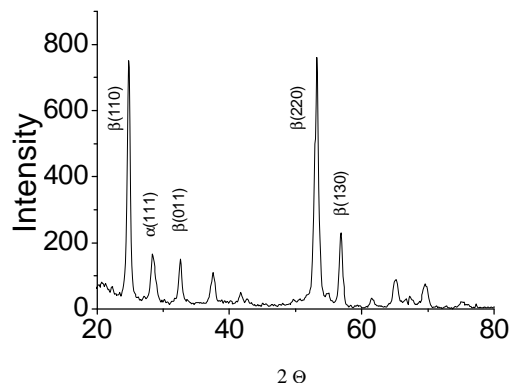


**Fig. 8a.** X-ray diffractograms of a pure  $\text{PbO}_2$  film deposited at anodic current density of  $5 \text{ mA/cm}^2$  from the solution of  $0.1 \text{ M HNO}_3 + 0.1 \text{ M Pb(NO}_3)_2$

The crystallographic orientation of lead dioxide in the composite material substantially changes. For instance, in case of  $\text{PbO}_2$ - $\text{ZrO}_2$  composites the  $\beta(110)$ ,  $\beta(220)$ , and  $\alpha(111)$  peaks decrease or almost vanish, whereas  $\beta(101)$ ,  $\beta(211)$ , and  $\alpha(200)$  peaks arise. For the deposits containing particles of inert oxide and surfactant, the peak intensity significantly decreases (Fig. 8b). This can be an evidence for a decrease in the dimensions of lead dioxide crystals with increasing fraction of amorphous phases in the composite. It should be noted that the X-ray diffraction patterns show no peaks of  $\text{TiO}_2$  and  $\text{ZrO}_2$ . Taking into account the very small average size of foreign oxide particles they are X-ray amorphous under the measurement conditions.

To obtain additional information, the surface morphology of the materials was studied by SEM. In electrodeposition of lead dioxide from nitrate solutions without additives [16], the coatings are composed of a set of coarse polycrystalline blocks with a poorly pronounced predominant orientation of separate faces (Fig. 9). As follows from the data obtained (Fig. 9), incorporation of foreign oxide particles into  $\text{PbO}_2$  results in a modified morphology of the deposit. The composite is a heterogeneous system composed of locally separated zones with different surface morphologies. The regions with coarse crystals are composed of lead dioxide particles, and those with fine crystals, of titanium dioxide or zirconium dioxide partly or completely covered with fine crystals of lead dioxide.

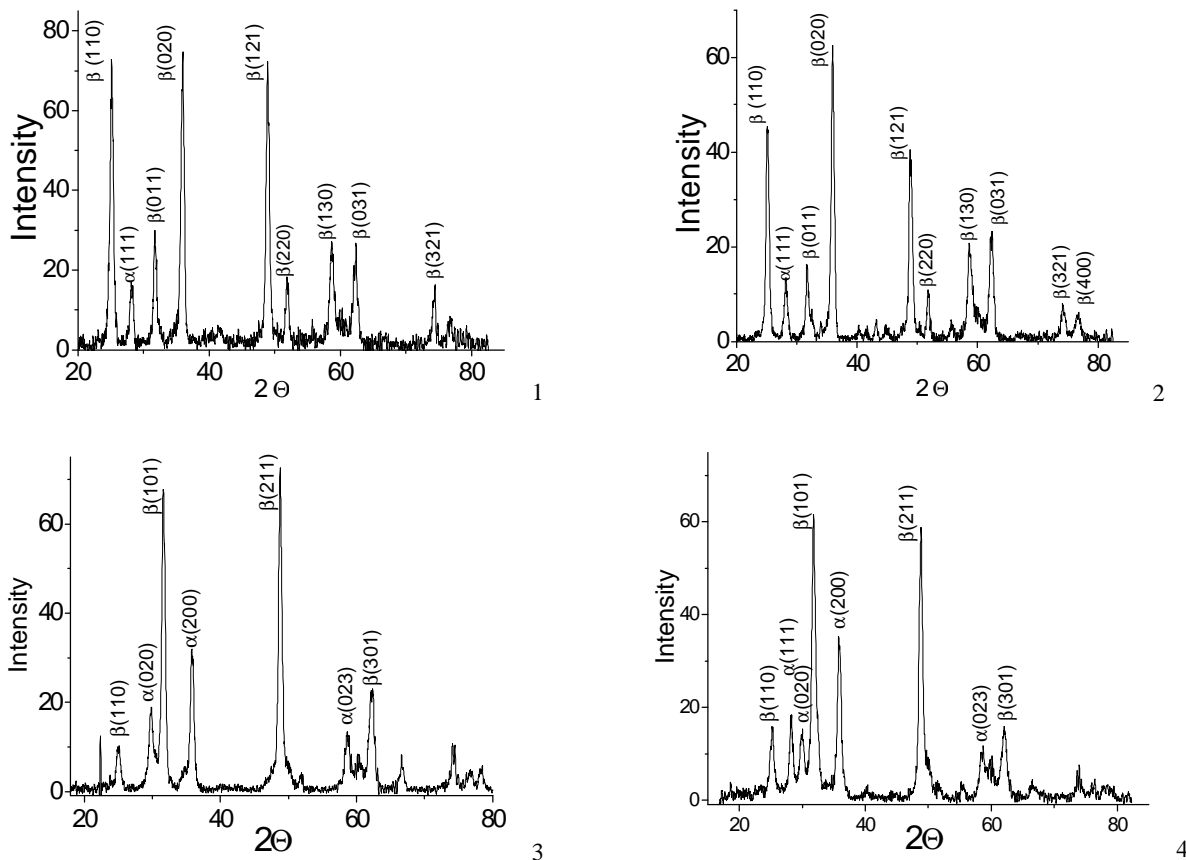


**Fig. 8b.** X-ray diffractograms of composites deposited at anodic current density of 5 mA/cm<sup>2</sup> from different solutions: 0.1M HNO<sub>3</sub> + 0.1M Pb(NO<sub>3</sub>)<sub>2</sub> + 2.0 g/dm<sup>3</sup> TiO<sub>2</sub> (1); 0.1M HNO<sub>3</sub> + 0.1M Pb(NO<sub>3</sub>)<sub>2</sub> + 2.0 g/dm<sup>3</sup> TiO<sub>2</sub> + 7·10<sup>-4</sup>M SDS (2); 0.1M HNO<sub>3</sub> + 0.1M Pb(NO<sub>3</sub>)<sub>2</sub> + 1.0 g/dm<sup>3</sup> ZrO<sub>2</sub> (3) and 0.1M HNO<sub>3</sub> + 0.1M Pb(NO<sub>3</sub>)<sub>2</sub> + 1.0 g/dm<sup>3</sup> ZrO<sub>2</sub> + 7·10<sup>-4</sup>M SDS (4)

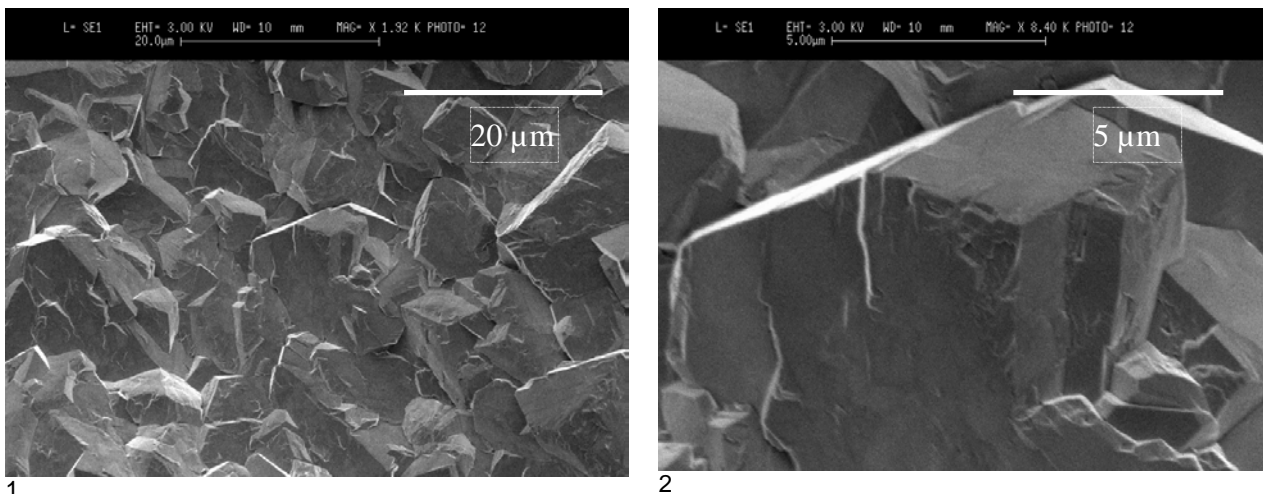


**Fig. 9.** SEM micrographs of composites deposited at anodic current density 5 mA/cm<sup>2</sup> from different solutions: 0.1M HNO<sub>3</sub> + 0.1M Pb(NO<sub>3</sub>)<sub>2</sub> (1, 2); 0.1M HNO<sub>3</sub> + 0.1M Pb(NO<sub>3</sub>)<sub>2</sub> + 2.0 g/dm<sup>3</sup> TiO<sub>2</sub> (3); 0.1M HNO<sub>3</sub> + 0.1M Pb(NO<sub>3</sub>)<sub>2</sub> + 2.0 g/dm<sup>3</sup> TiO<sub>2</sub> + 7·10<sup>-4</sup>M SDS (4); 0.1M HNO<sub>3</sub> + 0.1M Pb(NO<sub>3</sub>)<sub>2</sub> + 1.0 g/dm<sup>3</sup> ZrO<sub>2</sub> (5) and 0.1M HNO<sub>3</sub> + 0.1M Pb(NO<sub>3</sub>)<sub>2</sub> + 1.0 g/dm<sup>3</sup> ZrO<sub>2</sub> + 7·10<sup>-4</sup>M SDS (6)

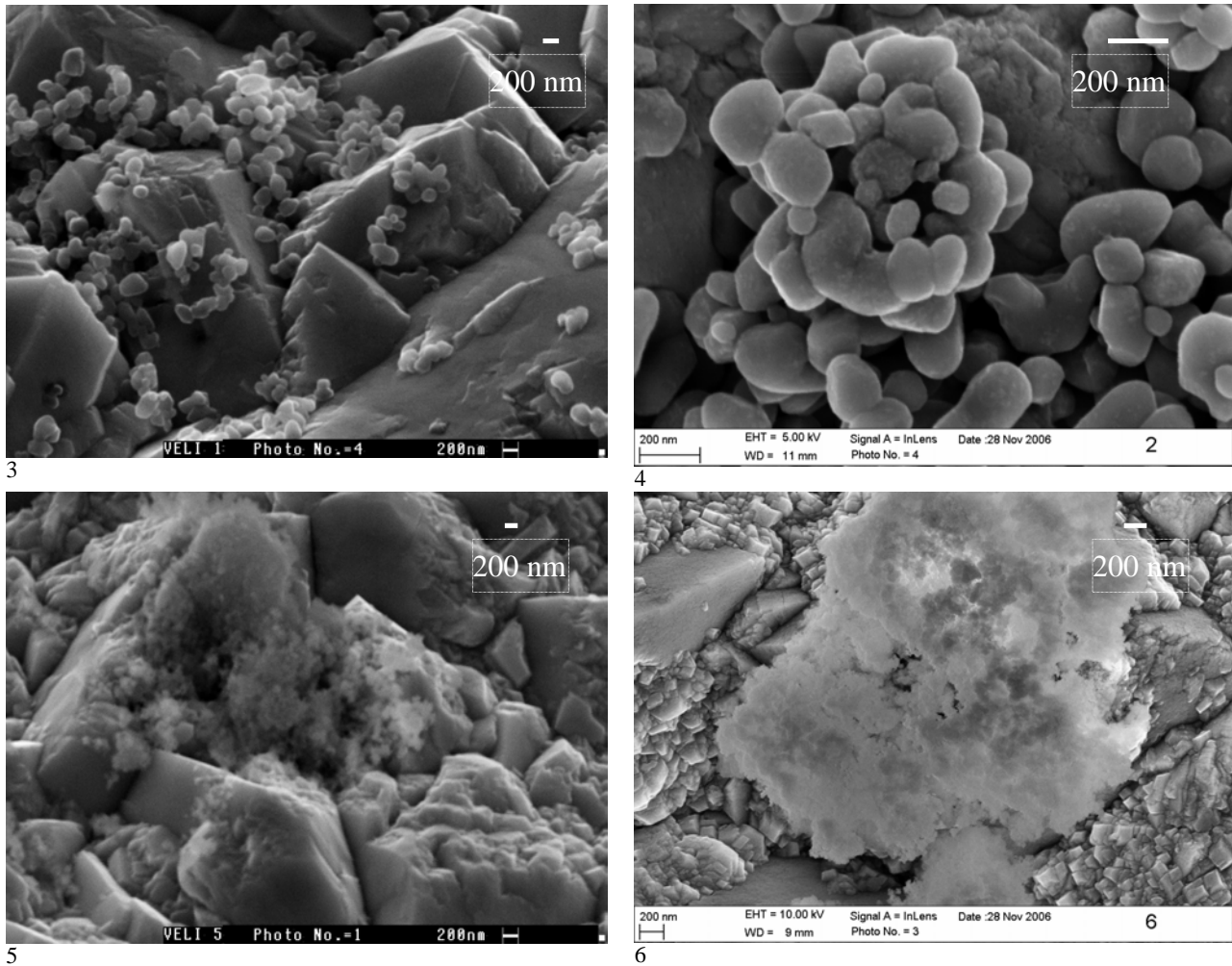
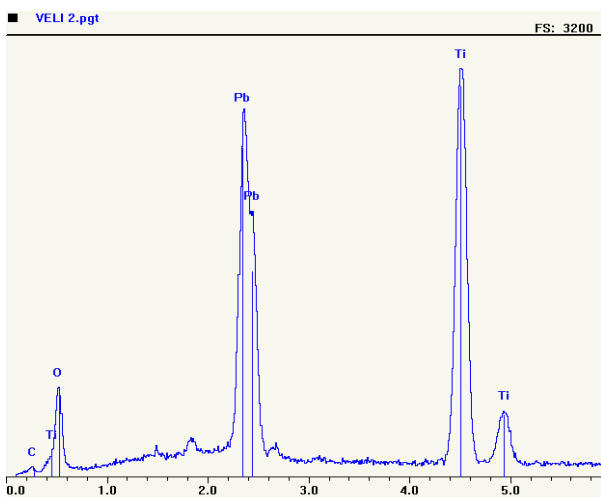
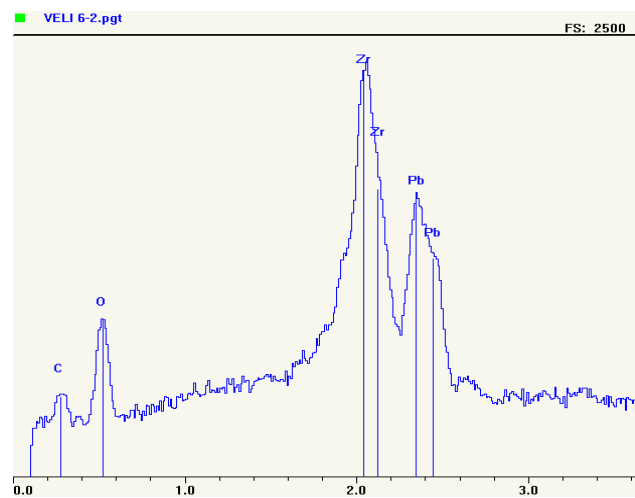


Fig. 9. Continuation



**Fig. 10a.** EDX data for the composite deposited at anodic current density of 5 mA/cm<sup>2</sup> from 0.1M HNO<sub>3</sub> + 0.1M Pb(NO<sub>3</sub>)<sub>2</sub> + 2.0 g/dm<sup>3</sup> TiO<sub>2</sub> + 7·10<sup>-4</sup>M SDS



**Fig. 10b.** EDX data for the composite deposited at anodic current density of 5 mA/cm<sup>2</sup> from 0.1M HNO<sub>3</sub> + 0.1M Pb(NO<sub>3</sub>)<sub>2</sub> + 1.0 g/dm<sup>3</sup> ZrO<sub>2</sub> + 7·10<sup>-4</sup>M SDS



This result is in agreement with the suggestion of involving TiO<sub>2</sub> and ZrO<sub>2</sub> in the electrochemical lead dioxide deposition due to Pb<sup>2+</sup> adsorption on the particles of the dispersed phase. The disappearance of coarse crystals and polycrystalline blocks, characteristic of lead dioxide, indicates that the number of crystallization centers grows as the TiO<sub>2</sub> or ZrO<sub>2</sub> content of the composite increases and that the additive is adsorbed on the electrode. Thus, the composite materials have the form of a PbO<sub>2</sub> matrix with sub-micrometer and nanosize crystals, into which TiO<sub>2</sub> and ZrO<sub>2</sub> crystals are incorporated.

### 3.4. Service Life and Oxygen Evolution on Composite Electrodes

Accelerated tests for determination of service life of anodes with an active layer of the PbO<sub>2</sub>-TiO<sub>2</sub> and PbO<sub>2</sub>-ZrO<sub>2</sub> composites were performed in 1 M H<sub>2</sub>SO<sub>4</sub> at an anode current density of 200 mA/cm<sup>2</sup>. The service life of the electrodes is determined by the time of uninterrupted polarization during which the potential remains nearly unchanged. A steep rise in the potential (a few volts) due to passivation of a titanium substrate indicates failure of an electrode, even though no mechanical damage of the active coating is visually observed. Such an electrode cannot be used because of the substantial increase in the electrolyzer voltage. As follows from the data obtained, electrodes containing 5.0 wt % titanium dioxide could operate during 207 h, and pure lead dioxide electrodes during only 105 h at the same current density. Thus, the service life of the composite materials increases approximately two times, compared with the conventional PbO<sub>2</sub> anodes. The same effect we observed for PbO<sub>2</sub>-ZrO<sub>2</sub> composites. It should be noted that lead dioxide electrodes are commonly used at current densities of 20–50 mA/cm<sup>2</sup> and it can be thought that in these modes the service life of the electrodes will be much longer [33, 34]. Thus, the composite materials obtained can be recommended for use as electrocatalysts with a prolonged service life.

Electrocatalytic activity of composite materials was studied for oxygen evolution reaction (OER). According to data presented in Fig. 11, overpotential of oxygen evolution at composite materials is much higher than at PbO<sub>2</sub> electrode.

It indicates a low electrocatalytic activity for OER. Our view on a possible mechanism is that the model of O<sub>2</sub> evolution on Pb/PbO<sub>2</sub> electrodes proposed by Pavlov and co-workers [17-19] can provide a reasonable explanation for the present data. According to that mechanism, O<sub>2</sub> evolution occurs at active sites located in a hydrous layer on PbO<sub>2</sub> whose structure and characteristics have been examined in [17-19]. According to their description, the surface consists of crystalline PbO<sub>2</sub> or hydrated

PbO·(OH)<sub>2</sub> zones which are in equilibrium, and the latter is a rather open structure which can exchange cations and anions. Oxygen evolution proceeds through the following elementary steps:

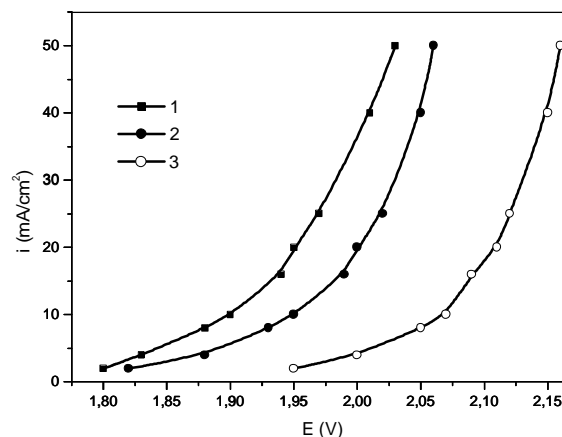
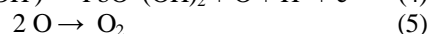
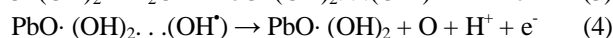
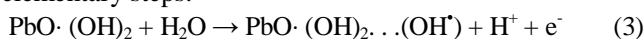


**Fig. 11.** Steady-state polarization curves in 1M H<sub>2</sub>SO<sub>4</sub> obtained with electrodes deposited at 5 mA/cm<sup>2</sup> from different solutions: 0.1M HNO<sub>3</sub> + 0.1M Pb(NO<sub>3</sub>)<sub>2</sub> (1); 0.1M HNO<sub>3</sub> + 0.1M Pb(NO<sub>3</sub>)<sub>2</sub> + 2.0 g/dm<sup>3</sup> TiO<sub>2</sub> (2) and 0.1M HNO<sub>3</sub> + 0.1 M Pb(NO<sub>3</sub>)<sub>2</sub> + 1.0 g/dm<sup>3</sup> ZrO<sub>2</sub> (3)

Oxygen evolution reaction at PbO<sub>2</sub> electrode in acidic solution is limited by a second electron transfer (4) [20], so called “oxygen electrochemical desorption” stage. In general case electrocatalytic activity of an electrode for any kind of oxygen-transfer reactions strongly depends on the bond strength of chemisorbed oxygen-containing particles on the electrode surface [21]. Since no *in situ* electrochemical data are available for oxides, the evolution of the electrocatalytic activity may be based on the experimental data taken from neighboring fields. Any step of the reaction of oxygen evolution can be envisaged as a transition of the underlying oxide to a higher state. This reason can also be viewed as a transition between two different configurations of the surface coordination complex or between two different complexes (the coordination number of the surface hydroxy-complex is increased by one). In this context, the parameter which is expected to parallel the energy change occurring during the electrochemical reaction is the enthalpy of the oxide transition from a lower to a higher oxidation state [21].

According to [21] one may judge the bond strength of the chemisorbed oxygen with the electrode surface from the standard enthalpy of lower → higher oxide transition. Increase of the enthalpy (Table 2) indicates an increasing bond strength of chemisorbed oxygen - containing particles on the electrode surface that leads to

inhibit OER in the sequence:  $\text{PbO}_2 < \text{PbO}_2\text{-TiO}_2 < \text{PbO}_2\text{-ZrO}_2$ , in good agreement with experimental data (Fig. 11).

Table 2

**Standard enthalpy of lower → higher oxide transition calculated from standard enthalpy of formation for individual oxides**

Oxide	Transition	$-\Delta H$ , kJ/mol
$\text{PbO}_2$	$\text{Pb}_3\text{O}_4 \rightarrow \text{PbO}_2$	447.15
$\text{TiO}_2$	$\text{Ti}_2\text{O}_3 \rightarrow \text{TiO}_2$	574.47
$\text{ZrO}_2$	$\text{Zr}_2\text{O}_3 \rightarrow \text{ZrO}_2$	707.40

### 3.5. Oxidation of MTBE on Composite Electrodes

The electrochemical degradation of organic pollutants present in wastewater is a very important problem to be solved; many papers are devoted to that subject and new anode materials have been investigated, for example boron doped diamond electrodes (BDD), although modified  $\text{PbO}_2$  anodes have also been proposed [6].

Methyl *tert*-butyl ether (MTBE) is one of the most widely used motor fuel additives. Despite its success in the improvement of fuel combustion efficiency and air quality, numerous corrosion failures have caused it to leak from fuel storage tanks and now MTBE has been widely found in both groundwater and surface waters [22-25]. Electrochemical conversion and degradation of organic pollutants offers benefits such as potentially high efficiency, availability of convenient process control options (*e.g.*, cell current, voltage and potential of working electrodes) and reagent-free operations that might result in lower costs of treatment. The chemical and electrochemical degradation of MTBE and many other organic pollutants can take place *via* the transfer of oxygen atoms from water molecules to the target molecules and their breakdown products. Transition metal oxide anodes, and most notably lead dioxide-based materials exhibit high electrocatalytic activity in electrochemical (EC) degradation of a number of recalcitrant organic pollutants, for instance 4-chlorophenol, 2,4-dichlorophenoxyacetic acid and others [26].

In this paper, we will examine the performance of  $\text{PbO}_2\text{-TiO}_2$  anodes in the EC degradation of MTBE. It is also relevant to mention that only very little information concerning EC oxidation of MTBE is available in the literature [27]. Gas chromatographic measurements showed that *tert*-butanol (TBA), acetone, acetic acid and  $\text{CO}_2$  were main by-products of electrochemical degradation of MTBE at  $\text{PbO}_2$  electrodes [55]. The concentration of TBA reached a maximum after 1 h of electrolysis, while the concentrations of acetone and acetic

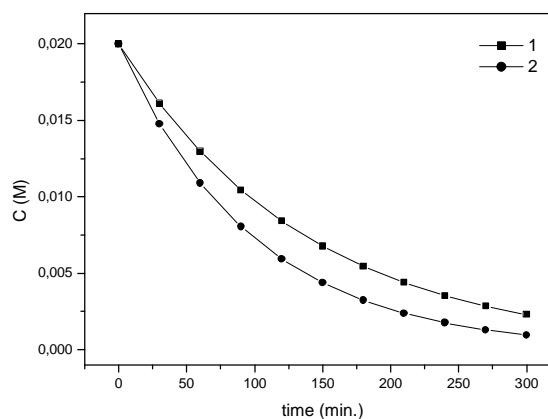
acid increased for treatment times of up to 3 h. After 6 h of electrolysis, only impurity level of acetic acid was found.

Table 3

**Kinetic parameters (constant rate  $k$ , and half-life  $t_{1/2}$ ) of electrochemical MTBE degradation at different  $\text{PbO}_2$  anodes**

Electrode material	$k$ , 1/min	$t_{1/2}$ , min
$\text{PbO}_2$	$5.5 \cdot 10^{-3}$	125
$\text{PbO}_2\text{-TiO}_2$ (6 wt %)	$7.0 \cdot 10^{-3}$	99
$\text{PbO}_2\text{-TiO}_2$ (16 wt %)	$1.0 \cdot 10^{-2}$	69
$\text{PbO}_2\text{-TiO}_2$ (6 wt. %) under UV irradiation	$1.2 \cdot 10^{-2}$	58
$\text{PbO}_2\text{-TiO}_2$ (16 wt. %) under UV irradiation	$1.2 \cdot 10^{-2}$	58

The disappearance of MTBE as a function of electrolysis time at anodic current density  $j = 50 \text{ mA/cm}^2$  at the  $\text{PbO}_2\text{-TiO}_2$  electrode is shown in Fig. 12.



**Fig. 12.** MTBE degradation during electrolysis at anodic current density  $j = 50 \text{ mA/cm}^2$  on  $\text{PbO}_2\text{-TiO}_2$  (6 wt %) composite anode: without UV-irradiation (1) and under UV-irradiation (2). Initial solution: 0.5M  $\text{Na}_2\text{SO}_4$  + phosphate buffer +  $2 \cdot 10^{-2}$ M MTBE (pH = 6.68)

According to our calculation performed on kinetic data (evolution of MTBE concentration vs time) electrochemical oxidation of MTBE is a pseudo first order reaction with main kinetic parameters presented in Table 3. It is important to note that increasing  $\text{TiO}_2$  content in composite electrodes leads to the rate increase of MTBE electrooxidation in two times (Table 3) with decreasing half-life of reaction from 125 to 69 min. The stronger electrocatalytic activity of composite  $\text{PbO}_2\text{-TiO}_2$  electrodes to some oxygen-transfer reaction may be linked to a larger amount of strongly-bonded oxygen-containing particles on the electrode surface.

Another interesting effect is the increase of MTBE electrooxidation rate under UV irradiation (Fig. 12, Table 3). In case of the composite containing 6 wt % of TiO<sub>2</sub> the constant rate of MTBE electrooxidation increases in two times under UV irradiation with decreasing of half-life of reaction from 99 to 58 min. We suggest that this effect is related to the additional generation of OH-radicals due to photocatalysis. Synergistic effects of irradiation in oxidation reactions at PbO<sub>2</sub>-TiO<sub>2</sub> electrodes have been previously observed [28, 29]. Some of these studies [29] have dealt with the degradation of dyes using UV illumination at 254 nm where, admittedly, the organic substrate absorbs light.

## 4. Conclusions

1. Use of suspension electrolytes makes it possible to obtain composite materials, *i.e.* lead dioxide matrixes into which an inert oxide is incorporated. Particles of the dispersed phase can be delivered to the electrode surface by convective-diffusion due to stirring of the suspensions. In addition, the effect of migration must be taken into account when SDS is added to the plating bath. The oxide of dispersed phase is involved in the electrochemical deposition of lead dioxide due to formation of extra nucleation sites like [MO<sub>2</sub>]Pb<sup>2+</sup><sub>ads</sub> or [MO<sub>2</sub>]OH<sub>ads</sub>. The amount of TiO<sub>2</sub> in the composite can vary from 3 to 16 wt % by changing the electrochemical deposition conditions and the electrolyte composition.

2. The physicochemical properties of the composites significantly differ from those of pure lead dioxide and are determined by the composition of these materials. The composites have the form of PbO<sub>2</sub> matrixes with submicrometer and nanosize crystals, into which TiO<sub>2</sub> or ZrO<sub>2</sub> particles are incorporated. Owing to this structure, the composites have a large effective surface area.

3. The service life of composite anodes is at least two times higher than that of pure lead dioxide. The electrocatalytic activity of the composites strongly depends on the amount and nature of the foreign oxide. It was shown that oxygen evolution overpotential and rate of MTBE electrooxidation increase at composite material electrodes. According to presented data, PbO<sub>2</sub>-TiO<sub>2</sub> and PbO<sub>2</sub>-ZrO<sub>2</sub> composite materials are interesting for industrial applications as electrocatalysts with good mechanical properties and long service life.

## References

- [1] Yeo I., Lee Y. and Johnson D.: *Electrochim. Acta*, 1992, **37**, 1811.
- [2] Casellato U., Cattarin S. and Musiani M.: *Electrochim. Acta*, 2003, **48**, 3991.
- [3] Cattarin S. and Musiani M.: *Electrochim. Acta*, 2006, **52**, 1339.
- [4] Amadelli R., Samiolo L., Velichenko A. *et al.*: *Electrochim. Acta*, 2009, **54**, 5239.
- [5] Amadelli R., Armelao L., Velichenko A. *et al.*: *Electrochim. Acta*, 1999, **45**, 757.
- [6] Amadelli R., De Battisti A., Girenko D. *et al.*: *Electrochim. Acta*, 2000, **46**, 341.
- [7] Velichenko A., Portillo J., Sarret M. and Muller C.: *Electrochim. Acta*, 1999, **44**, 3377.
- [8] Casellato U., Cattarin S., Guerriero P. and Musiani M.: *Chem. Mater.*, 1997, **9**, 960.
- [9] Cattarin S., Frateur I., Guerriero P. and Musiani M.: *Electrochim. Acta*, 2000, **45**, 2279.
- [10] Velichenko A., Girenko D., Kovalyov S. *et al.*: *J. Electroanal. Chem.*, 1998, **454**, 203.
- [11] Amadelli R., Samiolo L., De Battisti A. and Velichenko A.: *J. Electrochem. Soc.*, 2011, **158**, P87.
- [12] Kim J., Korshin G. and Velichenko A.: *Water Res.*, 2005, **39**, 2527.
- [13] Velichenko A. and Devilliers D.: *J. Fluorine Chem.*, 2007, **128**, 269.
- [14] Velichenko A., Amadelli R., Knysh V. *et al.*: *J. Electroanal. Chem.*, 2009, **632**, 192.
- [15] Velichenko A., Baranova E., Girenko D. and Danilov F.: *Russ. J. Electrochem.*, 2003, **39**, 615.
- [16] Velichenko A., Amadelli R., Benedetti A. *Et alF.*: *J. Electrochem. Soc.*, 2002, **149**, C445.
- [17] Pavlov D. and Monahov B.: *J. Electrochem. Soc.*, 1996, **143**, 3616.
- [18] Pavlov D. and Monahov B.: *J. Electrochem. Soc.*, 1998, **145**, 70.
- [19] Monahov B., Pavlov D. and Petrov D.: *J. Power Sources*, 2000, **85**, 59.
- [20] Amadelli R., Maldotti A., Molinari A. *et al.*: *J. Electroanal. Chem.*, 2002, **534**, 1.
- [21] Trasatti S.: *Electrochim. Acta*, 1984, **29**, 1503.
- [22] Chang P. and Young T.: *Water Res.*, 2000, **34**, 2233.
- [23] Safarzadeh-Amiri A.: *Water Res.*, 2001, **35**, 3706.
- [24] Bergendahl J. and Thies T.: *Water Res.*, 2004, **38**, 334.
- [25] Burbano A., Dionysiou D. and Suidan M.: *Water Res.*, 2008, **42**, 3225.
- [26] Johnson D., Feng J. and Houk L.: *Electrochim. Acta*, 2000, **46**, 323.
- [27] Wu T.: *Chemosphere*, 2007, **69**, 271.
- [28] Li G., Qu J., Zhang X. *et al.*: *J. Mol. Catal.*, 2006, **259**, 238.
- [29] Li J., Zheng L., Li L. *et al.*: *Electroanalysis*, 2006, **18**, 2251.

## КОМПОЗИЦІЙНІ МАТЕРІАЛИ НА ОСНОВІ PbO<sub>2</sub>, ЩО ОСАДЖЕНІ З СУСПЕНЗІЙНИХ ЕЛЕКТРОЛІТІВ: ЕЛЕКТРОСИНТЕЗ, ФІЗИКО-ХІМІЧНІ І ЕЛЕКТРОХІМІЧНІ ВЛАСТИВОСТІ

**Анотація.** Композиційні матеріали на основі PbO<sub>2</sub>, що мають в своєму складі TiO<sub>2</sub> або ZrO<sub>2</sub>, були одержані з суспензійних електролітів з часточками дисперсної фази TiO<sub>2</sub> чи ZrO<sub>2</sub>. Концентрація сторонніх оксидів в композиті залежить від складу електроліту та умов осадження. В процесі залучення часточок дисперсної фази до композиту кристали плюмбум(IV) оксиду зменшуються до субмікроних та нано-розмірів. Фізико-хімічні властивості та електрокаталітична активність композиційних матеріалів у більшості випадків обумовлюється їх хімічним складом. Досліджено електрокаталітичні властивості композиційних анодів PbO<sub>2</sub>-TiO<sub>2</sub> в реакціях виділення кисню та електрохімічного руйнування метил трет-бутилового етеру (MTBE).

**Ключові слова:** електроосадження, суспензія, композит, PbO<sub>2</sub>, TiO<sub>2</sub>, ZrO<sub>2</sub>, MTBE.